THE ASTROPHYSICAL JOURNAL, 514:869–877, 1999 April 1

MICROLENS PARALLAXES WITH SIRTF

ANDREW GOULD[1]
Ohio State University, Department of Astronomy, 174 West 18th Avenue, Columbus, OH 43210; gould@astronomy.ohio-state.edu
Received 1998 July 27; accepted 1998 November 2

ABSTRACT

The Space Infrared Telescope Facility (SIRTF) will drift away from the Earth at ~ 0.1 AU yr^{-1}. Microlensing events will therefore have different characteristics as seen from the satellite and the Earth. From the difference it is possible in principle to measure $\tilde{\boldsymbol{v}}$, the transverse velocity of the lens projected onto the observer plane. Since $\tilde{\boldsymbol{v}}$ has very different values for different populations (disk, halo, Large Magellanic Cloud), such measurements could help identify the location, and hence the nature, of the lenses. I show that the method previously developed by Gould for measuring such satellite parallaxes fails completely in the case of SIRTF: it is overwhelmed by degeneracies that arise from fact that the Earth and satellite observations are in different bandpasses. I develop a new method that allows for observations in different bandpasses and yet removes all degeneracies. The method combines a purely ground-based measurement of the "parallax asymmetry" with a measurement of the delay between the time the event peaks at the Earth and satellite. In effect, the parallax asymmetry determines the component of $\tilde{\boldsymbol{v}}$ in the Earth-Sun direction, while the delay time measures the component of $\tilde{\boldsymbol{v}}$ in the direction of the Earth's orbit.

Subject headings: dark matter — Galaxy: halo — gravitational lensing — Magellanic Clouds

1. INTRODUCTION

Over a dozen candidate microlensing events have been discovered toward the Large Magellanic Cloud (LMC) (Aubourg et al. 1993; Alcock et al. 1997a). They have typical Einstein crossing times, $t_e \sim 40$ days. Here t_e is related to the Einstein radius, r_e, by

$$t_e \equiv \frac{r_e}{|\boldsymbol{v}|}\,, \quad r_e^2 = \frac{4GMd_{\rm ol}\,d_{\rm ls}}{d_{\rm os}\,c^2}\,, \tag{1}$$

where $\boldsymbol{v}$ is the transverse velocity of the lens relative to the observer-source line of sight, M is the mass, and $d_{\rm ol}$, $d_{\rm ls}$, and $d_{\rm os}$ are the distances between the observer, lens, and source. If the lenses are assumed to be in the Galactic halo, they would appear to make up of order half the dark matter and have typical masses of $M \sim 0.4\,M_\odot$ (Alcock et al. 1997a). Several lines of reasoning suggest that this interpretation is implausible. However, to date there are no plausible alternatives.

The halo cannot be composed of $M \sim 0.4\,M_\odot$ hydrogen objects, or they would burn and would easily be detected. If it were composed of white dwarfs, the white dwarfs themselves, their progenitors at high redshift, and the metals these produce would all be detectable in various ways (Fields, Freese, & Graff 1998). The most viable candidates for halo lenses seem to be exotic new objects such as primordial black holes, which just happen to have the same masses as the most common stars. In addition, if halo objects are causing events toward the LMC, they should also generate events of similar duration and frequency toward the Small Magellanic Cloud (SMC). However, the only two events discovered toward the SMC to date show significant evidence of being due to SMC lenses (Palanque-Delabrouille et al. 1998; Afonso et al. 1998; Alcock et al. 1997c, 1997a; Albrow et al. 1999; Udalski et al. 1998).

On the other hand, if the LMC lensing events were due to lenses in the LMC bar/disk itself (Sahu 1994; Wu 1994), then the event rate should be much lower than observed (Gould 1995b), and their distribution on the sky should be more concentrated toward the bar (Alcock et al. 1997a). If they were due to a tidally disrupted dwarf galaxy along the line of sight to the LMC (Zhao 1998; Zaritsky & Lin 1998), they should be observable in surface brightness maps (Gould 1998a) and tracer populations like RR Lyrae stars (Alcock et al. 1997b) and clump giants (Bennett 1998). Hence there are no compelling candidates for the lens population.

The different possible lens populations have radically different kinematics, and one could therefore distinguish among them if kinematic parameters could be measured. This is not possible for most events, because the one measured quantity, t_e, is a combination of the mass, distance, and speed (see eq. [1]). However, if a satellite were launched into solar orbit, the event would appear differently from the satellite than from the Earth. From the difference, one could in effect measure the length of time it takes for the projected position of the lens to travel from the Earth to the satellite and also its direction of transverse motion. Since the distance between the Earth and satellite is known, one could thereby determine the two components of the transverse velocity projected onto the plane of the observer,

$$\tilde{\boldsymbol{v}} = \frac{d_{\rm os}}{d_{\rm ls}}\,\boldsymbol{v}\,. \tag{2}$$

Since $\tilde{v} \equiv |\tilde{\boldsymbol{v}}|$ has values of ~ 50 km s^{-1} for disk lenses, ~ 275 km s^{-1} for halo lenses, and $\gtrsim 1000$ km s^{-1} for LMC lenses, measurement of this quantity should distinguish well among components.

2. DEGENERACIES

Within the framework originally formulated by Refsdal (1966) and Gould (1994), the parallax-satellite measurement of $\tilde{\boldsymbol{v}}$ was subject to a fourfold degeneracy, including a twofold degeneracy in $\tilde{v}$. These degeneracies can be understood as follows. For any given observer (Earth or satellite), the magnification $A(u)$ is a function only of the projected

[1] Alfred P. Sloan Foundation Fellow.

lens-source separation u (Paczyński 1986),

$$A(u) = \frac{u^2 + 2}{u(u^2 + 4)^{1/2}}, \quad u(t) = \left[\left(\frac{t - t_0}{t_e}\right)^2 + \beta^2\right]^{1/2}, \quad (3)$$

where t_0 is the time of maximum magnification, and β is the impact parameter. In units of the projected Einstein ring, $\tilde{r}_e = (d_{os}/d_{ls})r_e$, the separation between the Earth and the satellite along the direction of the lens motion is simply $\Delta t_0/t_e$, where

$$\Delta t_0 \equiv t_{0,S} - t_{0,\oplus} \quad (4)$$

is the difference in the observed times of maximum. However, the separation in the direction normal to the lens motion (in units of $\tilde{r}_e$) has four possible values, $\pm\Delta\beta_+$ and $\pm\Delta\beta_-$, where $\Delta\beta_\pm = |\beta_S \pm \beta_\oplus|$. Since

$$\tilde{\boldsymbol{v}} \cdot \Delta\boldsymbol{u} = \frac{d}{t_e}, \quad \Delta\boldsymbol{u} \equiv \left(\frac{\Delta t_0}{t_e}, \Delta\beta\right), \quad (5)$$

this engenders a fourfold degeneracy in $\tilde{\boldsymbol{v}}$ in direction and a twofold degeneracy in amplitude. Here d is the Earth-satellite distance.

It is, however, possible to break this degeneracy by taking advantage of the fact that the velocities of the Earth and satellite differ in the $\Delta\beta$ direction, leading to a difference in observed timescales, $\Delta t_e = 2\pi\ \mathrm{yr}^{-1}\ \Delta\beta t_e^2$, where $\Delta t_e \equiv t_{e,S} - t_{e,\oplus}$ and where I have adopted the conventions that the satellite is trailing the Earth and that if $\tilde{\boldsymbol{v}}$ is outward from the Sun, then $\Delta\beta > 0$. Hence, if this time difference can be measured, $\Delta\beta$ can be unambiguously determined (Gould 1995a):

$$\Delta\beta = \frac{1}{\Omega_\oplus t_e}\frac{\Delta t_e}{t_e}, \quad \Omega_\oplus \equiv \frac{2\pi}{\mathrm{yr}} \sim (58\ \mathrm{days})^{-1}. \quad (6)$$

However, measurement of the timescale difference introduces an additional degeneracy that must be dealt with very carefully. The observed flux from the star is actually a function of five parameters:

$$F(t; t_0, \beta, t_e, F_0, B) = F_0\, A[u(t; t_0, \beta, t_e)] + B, \quad (7)$$

where F_0 is the source flux, and B is any background light that falls into the aperture but is not lensed. Measurement of B is highly correlated both with β and t_e, because the effect on the light curve of changing these three parameters is even in $(t - t_0)$ and all are very similar to one another. Hence it is all but impossible to measure the small timescale difference between the Earth and the satellite if each light curve is fitted with its own background parameter, B. When I proposed this method (Gould 1995a), I therefore explicitly assumed that the background light was identical for the two sources, $B_S \equiv B_\oplus$. Physically this condition can be attained if the filters have identical (or nearly identical) transmission properties and if the images are convolved to the same seeing. With this constraint, $t_{e,S}$ is still highly correlated with B_S, and $t_{e,\oplus}$ is highly correlated with $B_\oplus$. However, since $B_S = B_\oplus$, the difference $\Delta t_e \equiv t_{e,S} - t_{e,\oplus}$ is well constrained.

The Space Infrared Telescope Facility (SIRTF) will be launched into solar orbit early in the next decade and will drift away from the Earth at $\sim$0.1 AU yr^{-1}. In this respect, it is in an excellent position to measure microlens parallaxes. However, the bluest band it can observe is the L band ($\sim$3.6 μm). Because of the complexity of atmospheric transmission at L, it is not possible to mimic the space-based detector response from the ground. Moreover, the ground-based background in L is so high that it is not practical to monitor typical LMC sources ($V \gtrsim 20$) from the ground. Hence one cannot ensure $B_S = B_\oplus$, so it is not possible for SIRTF to measure parallaxes using my original single-satellite approach (Gould 1995a).

3. A NEW PARALLAX METHOD

To recapitulate, SIRTF has no trouble measuring one component of $\Delta\boldsymbol{u}$, namely Δt_0, which is unambiguously given by the difference in times of peak magnifications. However, it cannot measure the other component, $\Delta\beta$, either directly or through measurement of Δt_e (via eq. [6]), because both parameters are degenerate with the blended light, B. The key to resolving this problem is to notice that equation (6) arises from the Earth-satellite velocity difference in the $\Delta\beta$ direction. However, the Earth itself undergoes a velocity change in this direction during the course of the event by an amount $\Delta v \sim \Omega t_e v_\oplus$, where $v_\oplus = 30$ km s^{-1} is the speed of the Earth. This purely ground-based parallax effect leads to an asymmetry in the light curve that can, in effect, be used to measure $\Delta\beta$ and hence complete the measurement of $\Delta\boldsymbol{u}$.

Actually, such parallax asymmetries have a long history. I showed that for events of sufficiently long duration it would be possible to measure a complete parallax from the ground (Gould 1992). One such parallax measurement has been published for a long event ($t_e \sim 110$ days) seen toward the bulge (Alcock et al. 1995) and several others have been observed (Bennett et al. 1997). For shorter events ($\Omega_\oplus t_e \lesssim 1$), the acceleration of the Earth can be approximated as constant over the course of the event. Equation (3) is then replaced by (Gould, Miralda-Escudé, & Bahcall 1994)

$$u(t; t_0, \beta, t_e, \gamma) = \left\{\left[\xi\left(\frac{t - t_0}{t_e}\right)\right]^2 + \beta^2\right\}^{1/2},$$

$$\xi(y) = y + \frac{1}{2}\gamma y^2, \quad (8)$$

where

$$\gamma = \frac{v_\oplus}{\tilde{v}}\Omega_\oplus t_e \cos\phi, \quad (9)$$

ϕ is the angle between $\boldsymbol{v}$ and the Earth-Sun separation, and where I have made use of the fact that the LMC is approximately at the ecliptic pole. Gould et al. (1994) noted that even for very short events, halo lenses ($\tilde{v} \sim 275$ km s^{-1}) could be distinguished from disk lenses ($\tilde{v} \sim 50$ km s^{-1}), at least statistically. The problem is that in any individual case, if γ were measured to be consistent with zero, one would not know whether the lens were in the halo (where $\tilde{v}$ is large) or in the disk (and cos ϕ just happened to be small). Moreover, the principal question about the location of the lenses is not halo versus disk but halo versus LMC. For short events it would be extremely difficult to distinguish between halo and LMC lenses using this technique, even statistically.

However, the typical events observed toward the LMC now turn out to be considerably longer, $t_e \sim 40$ days. Indeed, their long timescale is a major puzzle. Hence I recently proposed that LMC events be intensively monitored to search for this effect (Gould 1998b). I showed that

one could distinguish statistically between the halo-lens and LMC-lens scenarios by observing 15–30 events over 5 yr. The Global Microlensing Alert Network collaboration (Alcock et al. 1997d) is routinely monitoring LMC events but probably not intensively enough to detect this effect. In any event, the fact that one measures only the degenerate combination, $\tilde{v}$ sec ϕ, and not the two parameters separately, means that one cannot resolve the nature of the events on an individual basis.

3.1. *Overview*

The new approach is to combine a ground-based measurement of γ (and of course $t_{0,\oplus}$) with a space-based measurement of $t_{0,S}$ (and therefore Δt_0) to completely determine $\Delta\boldsymbol{u}$. With this is mind, I write $\boldsymbol{u}$ in a basis that is rotated relative to equation (5),

$$\Delta\boldsymbol{u} = (\Delta u_x, \Delta u_y)\ , \quad \Delta u_x = \frac{\Delta t_0}{t_e}\cos\theta + \Delta\beta\sin\theta\ ,$$

$$\Delta u_y = -\frac{\Delta t_0}{t_e}\sin\theta + \Delta\beta\cos\theta\ . \tag{10}$$

Here Δu_x and Δu_y are antiparallel and outward normal to the direction of the Earth's motion at the midpoint of the event, while Δt_0 and $\Delta\beta$ are antiparallel and normal to the satellite-Earth separation vector. The rotation angle θ is defined by

$$\sin\theta \equiv \frac{d}{2\ \mathrm{AU}}\ . \tag{11}$$

This is convenient, because Δu_y can be simply expressed in terms of observables (see eqs. [5] and [9]),

$$\Delta u_y = \frac{d}{\mathrm{AU}}\,(\Omega_\oplus t_{e,\oplus})^{-2}\gamma_\oplus\ . \tag{12}$$

From both a conceptual and a practical point of view, it is useful to think of the measurement process as first determining the four Earth parameters, $t_{0,\oplus}$, $\beta_\oplus$, $t_{e,\oplus}$, and $\gamma_\oplus$, then using these to predict the four analogous satellite quantities as a function of the (unknown) parameter Δu_x :

$$t_{0,S} = t_{0,\oplus} + \Delta t_0\ ,$$

$$\frac{\Delta t_0}{t_{e,\oplus}} = \Delta u_x\cos\theta - 2(\Omega_\oplus t_{e,\oplus})^{-2}\gamma_\oplus\sin^2\theta\ ; \tag{13}$$

$$\beta_S = |\beta_\oplus \pm \Delta\beta|\ , \quad \Delta\beta = \Delta u_x\sin\theta + (\Omega_\oplus t_{e,\oplus})^{-2}\gamma_\oplus\sin 2\theta\ ; \tag{14}$$

$$t_{e,S} = t_{e,\oplus} + \Delta t_e\ ,$$

$$\frac{\Delta t_e}{t_{e,\oplus}} = \Delta u_x\Omega_\oplus t_{e,\oplus}\sin\theta + (\Omega_\oplus t_{e,\oplus})^{-1}\gamma_\oplus\sin 2\theta\ ; \tag{15}$$

$$\gamma_S = \Delta u_x(\Omega_\oplus t_{e,\oplus})^2\cos\theta + \gamma_\oplus\cos 2\theta\ . \tag{16}$$

The satellite measurements are then used to determine Δu_x.

Equations (14) and (15) yield very little information about Δu_x because β and t_e are poorly determined, being strongly correlated with B. In addition, equation (14) is ambiguous because in the limit $\Omega_\oplus t_e \lesssim 1$, the ground-based observations do not yield information about whether the lens passed on the satellite side or the opposite side of the Earth. Thus equation (14) contains essentially no information about Δu_x. It is not immediately obvious, but I show in § 3.2 that equation (16) also has relatively little information about Δu_x. Hence, in agreement with our naive expectation, Δu_x is mainly determined by measuring Δt_0. However, from equation (13) we see that uncertainties in the measurement of $\gamma_\oplus$ can propagate into the Δu_x determination.

3.2. *Ground-based Observations*

I have previously discussed in some detail the problem of early identification and intensive monitoring of microlensing events toward the LMC (Gould 1998b). As in that paper, I evaluate the covariance matrix c_{ij} of the six parameters $a_i(=t_0,\ \beta,\ t_e,\ \gamma,\ F_0,\ B)$ specified in equations (3), (7), and (8), by considering a series of measurements at times t_k and with errors σ_k,

$$c = b^{-1}\ , \quad b_{ij} = \sum_k \sigma_k^{-2}\,\frac{\partial F(t_k)}{\partial a_i}\,\frac{\partial F(t_k)}{\partial a_j}\ . \tag{17}$$

After taking the derivatives $\partial F(t_k)/\partial a_i$, I evaluate them assuming $B = \gamma = 0$. I assume that the errors are photon limited, i.e., $\sigma_k = \sigma_0 F_0[A(t_k)]^{1/2}$. (This assumption differs somewhat from Gould 1998b.) I assume that these intensive observations are triggered when the event enters the Einstein ring ($u_{\rm init} = 1$, $A(u_{\rm init}) = 1.34$) and end at $t = t_0 + 1.5t_e$, and they are carried on uniformly at a rate of N per day in the interval. I then find an uncertainty in the determination of all parameters. In particular, for the key parameters t_0, γ, and β, I find

$$\frac{\sigma_{t_0}}{t_e} = \frac{\sigma_0}{(Nt_e/\mathrm{day})^{1/2}}\,R(\beta)\ , \tag{18}$$

and

$$\sigma_\gamma = \frac{\sigma_0}{(Nt_e/\mathrm{day})^{1/2}}\,S(\beta)\ , \quad \sigma_\beta = \frac{\sigma_0}{(Nt_e/\mathrm{day})^{1/2}}\,T(\beta)\ , \tag{19}$$

where $R(\beta)$, $S(\beta)$, and $T(\beta)$ are shown in Figure 1.

These results shed light on three questions regarding equations (12), (13), and (16). First, the ratio of the contributions of σ_γ and σ_{t_0} to the error in the determination of Δu_x from equation (13) is

$$2(\Omega_\oplus t_e)^{-2}\sin^2\theta\,\frac{\sigma_\gamma}{\sigma_{t_0}/t_e} \simeq 0.4\left(\frac{d}{0.2\ \mathrm{AU}}\right)^2\left(\frac{t_e}{40\ \mathrm{days}}\right)^{-2}\frac{S(\beta)}{10R(\beta)}\ . \tag{20}$$

Thus, for typical parameters, the two sources of error are comparable. See Figure 1.

Second, I note that the error in Δu_x induced by the "$\gamma_\oplus$" term in equation (16) is larger than the error induced by the "Δt_0" term in equation (13) by a factor of $\sim S(\beta)/R(\beta) \sim 10$. Hence for typical parameters Δu_x is constrained primarily by equation (13). This result has the important consequence that the SIRTF observations should be optimized to constrain $t_{0,S}$ rather than γ_S or any other parameters (see § 3.3).

Finally, the error in Δu_y is larger by a factor of $\sim 2(d/\mathrm{AU})^{-1}$ than the error induced by the $\gamma_\oplus$ term in equation (13). By equation (20) the latter is comparable with the total error in Δu_x. Hence the (purely ground-based) error in Δu_y is substantially larger than the ground-based contribution to Δu_x. That is, the limit imposed by the ground-based observations on the overall precision of the measurement is

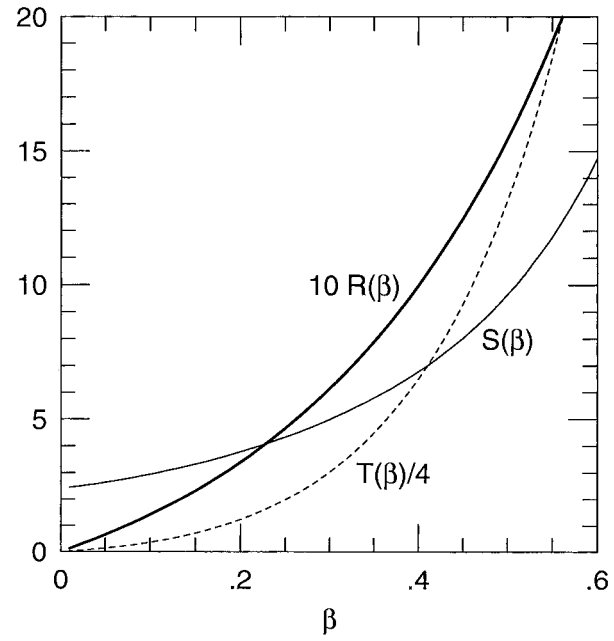

FIG. 1.—Normalized errors, R (*bold line*), S (*solid line*), and T (*dashed line*), for the measurements of t_0, β, and γ. These are, respectively, the time of maximum, the impact parameter, and the asymmetry parameter. Each is plotted as a function of the impact parameter, β. The actual error is given by, for example, $\sigma_\gamma = S\sigma_0/(Nt_e/\mathrm{day})^{1/2}$, where σ_0 is the factional flux error for an individual measurement, and (Nt_e/day) is the number of measurements per Einstein crossing time. These curves assume that light-curve measurements begin when the source enters the Einstein ring ($u_i = 1.0$) and end at $t = t_0 + 1.5t_e$.

set by the ground-based measurement of Δu_y, i.e., γ. From equations (9), (12), and (19), the error in Δu_y expressed as a fraction of Δu is

$$\frac{\sigma_{\Delta u_y}}{\Delta u} = \frac{\sigma_\gamma}{\gamma \sec\phi} = 0.17 N^{-1/2} \frac{\sigma_0}{0.01} \frac{\tilde{v}}{275 \text{ km s}^{-1}} \left(\frac{t_e}{40 \text{ days}}\right)^{-3/2} \frac{S(\beta)}{8} . \quad (21)$$

Thus for a robust detection of parallax for a halo event with typical parameters requires $\sigma_0 = 1\%$ photometry, on average once per day.

3.3. *SIRTF Observations*

There are a number of constraints that affect SIRTF observations that do not affect ground-based observations, the most important of which is scheduling. While the operational plan for SIRTF is not finalized, it is expected that the Infrared Array Camera (used for L-band photometry) will share time equally with two other instruments, rotating, for example, 1 week on, 2 weeks off. Thus the type of schedule envisaged for the ground-based observations (exposures once or several times per day) are out of the question for SIRTF. Instead, observations must be concentrated in a few critical periods, each less than a week and separated by several weeks. This appears at first to pose major difficulties, but in fact such constraints are perfectly compatible with an optimal observing plan.

To devise an optimal strategy, first recall that the flux is a function of time and six parameters, $F(t; a_i)$. The derivatives of this flux with respect to the parameters $\partial F/\partial a_i$ are even in $(t - t_0)$ for four parameters ($a_i = \beta, t_e, F_0, B$) and odd for the other two ($a_i = t_0, \gamma$). Hence, any set of observations that was symmetric in $(t - t_0)$ would automatically decouple the errors in (β, t_e, F_0, B) from those in (t_0, γ). This would be good, because from the discussion in §§ 3.1 and 3.2, t_0 and γ provide essentially all of the useful information. I focus first on the simplest symmetric case, two observations placed at $t_\pm = t_0 \pm \tau t_e$, where τ is a parameter. In fact, a third observation is required to establish the baseline, $F_0 + B$. I will return to this point below, but for the moment I assume that the baseline is known with perfect precision.

Now if it were literally true that there was *no* information about β, t_e, and $F_0 - B$, then of course a light-curve fit to only two points would be completely unconstrained. However, from the ground-based data and equations (14) and (15), β_S and $t_{e,S}$ are reasonably constrained. I will discuss this in more detail below. Here I focus on what specifically can be learned about $t_{0,S}$ and γ_S from this symmetric pair of observations. The (2×2) inverse covariance matrix associated with t_0 (normalized to t_e) and γ is (see eqs. [3], [7], and [17])

$$b_{ij}\left(\frac{t_0}{t_e}, \gamma\right) = \frac{64}{u^5(u^2+4)^{5/2}(u^2+2)\sigma_0^2} \begin{pmatrix} 2\tau^2 & -\tau^4 \\ -\tau^4 & \tau^6/2 \end{pmatrix} , \quad (22)$$

where $u^2 = \tau^2 + \beta^2$. This matrix is of course degenerate between t_0 and γ. I assume for the moment that the information in equation (16) is sufficient to break this degeneracy. (I check this assumption below.) The error in t_0/t_e from these two measurements is then $\sigma_{t_0} \simeq [b(1, 1)]^{-1/2}$. This error is minimized approximately at $\tau \sim (2/3)^{1/2}\beta$, at which point

$$\frac{\sigma_{t_0}}{t_e} \sim \left(\frac{25}{12}\right)^{1/2} \beta\sigma_* , \quad \sigma_* = \left(\frac{5}{3}\right)^{1/4} \beta^{1/2}\sigma_0 \left[\text{at } \tau = \left(\frac{2}{3}\right)^{1/2}\beta\right], \quad (23)$$

where σ_* is the approximate fractional flux error of the two observations and where I have made the evaluations using the approximation $A(u) \sim u^{-1}$. Thus for typical values, $\beta \sim 0.4$ and $t_e \sim 40$ days, the two observations are separated by ~ 26 days, and the error in t_0 is $\sigma_{t_0}/t_e \sim 0.6\sigma_*$.

3.4. *Correlations*

To arrive at this estimate, I have argued or assumed that one can ignore the numerous correlations among the 12 observable parameters (six from the Earth and six from the satellite). I test these assumptions by simulating a fit based on the observations as outlined in §§ 3.2 and 3.2. In order to do so, I must choose a relative scale of errors for the Earth and satellite observations. The observations should be designed so that the errors in Δu_x and Δu_y are roughly comparable. On the assumption that $[b(1, 1)]^{-1/2}$ in equation (23) gives a good estimate of the error in t_0 and that this error dominates the error in Δu_x (see eq. [13]), I initially assume that $(25/12)^{1/2}\beta\sigma_* = (d/\mathrm{AU})(\Omega_\oplus t_e)^{-2}\sigma_\gamma$ (see eq. [12]). For definiteness, I initially assume $d = 0.2$ AU and $t_{e,\oplus} = 40$ days.

I fitted for a total of 13 parameters, including 12 observables ($a_i, i = 1 \ldots 6$ for t_0, β, t_e, F_0, B, and γ as seen from the Earth and $a_i, i = 7 \ldots 12$ for same parameters as seen from the satellite) plus $a_{13} = \Delta u_x$, which is a derived parameter.

The inverse covariance matrix b_{ij} is given by the sum of four types of terms. First, there are terms of the form given by equation (17) for Earth-based observations that affect b_{ij}, $i, j = 1 \ldots 6$. Second, there are terms of the same form for satellite-based observations that affect b_{ij}, $i, j = 7 \ldots 12$. Third, there are contributions to b_{ij} from the constraints (13), (15), and (16). Each of these can be written in the form $\sum_i \alpha_i a_i = 0$. For example, for equation (16), $\alpha_{12} = 1$, $\alpha_{13} = -(\Omega_\oplus t_{e,\oplus})^{-2} \cos\theta$, $\alpha_6 = -\cos 2\theta$, and $\alpha_i = 0$ for all other i. These constraints lead to contributions to b_{ij} of the form $\alpha_i \alpha_j / Q^2$, where Q is an arbitrarily small number. Finally, equation (14) leads to a similar constraint, except that there is a discrete uncertainty in the sign of $\Delta\beta$. Hence the constraint is less certain and so has the form $\alpha_i \alpha_j / (\Delta\beta)^2$. For definiteness, I choose $\Delta\beta = 5\ \sigma_{\Delta u_y}$ on the assumption that the observations have been structured to detect $\Delta\beta$ at the 5 σ level.

I then find for a pair of observations that are exactly symmetric about $t_{0,S}$ that for $\beta = 0.1 \ldots 0.5$ the errors are higher than my naive expectations by factors of $f = 1.03$ 1.07, 1.14, 1.24, and 1.36. If the various assumptions that I have made in the analytic derivation had all held exactly, these ratios would all be unity. The deviations from unity are partly accounted for by the fact that to derive equation (23), I evaluated equation (22) assuming $(u^2 + 4)^{5/2}(u^2 + 2)/64 = 1$, whereas it is actually slightly higher and increases with increasing β. Another factor is that in equation (22), $[b(2, 2)/b(1, 1)]^{1/2} = \beta^2/3$. Thus as β increases the role of the $b(2, 2)$ (γ) term is relatively less well constrained by equation (16). In brief, the estimate (eq. [23]) for the required photometric precision is basically accurate but is slightly too optimistic for $\beta \gtrsim 0.3$.

However, the assumption that the pair of observations is *exactly* symmetric about $t_{0,S}$ is too idealized. Even if one had perfect freedom to schedule the observations and even if one knew $t_{0,\oplus}$, $t_{e,\oplus}$, and $\gamma_\oplus$ exactly from the ground-based observations, according to equation (13) there would still be an uncertainty of $\Delta u_x t_{e,\oplus} \cos\theta$ in the predicted value of Δt_0 (and so of $t_{0,S}$), where Δu_x is an unknown quantity still to be measured. For typical parameters, $\Delta t_0 \sim d/\tilde{v} \sim \mathcal{O}(1$ day). In addition, at the time that the second observation is planned, there will be some measurement uncertainties in $t_{0,\oplus}$, $t_{e,\oplus}$, and $\gamma_\oplus$. This will lead to an additional uncertainty in the prediction of $t_{0,S}$, although this uncertainty will probably be less than 1 day. The biggest potential problem is that it may not be possible to schedule the second set of observations exactly when one would like.

Regardless of the reason, if the observations are not symmetric about $t_{0,S}$, then the errors in β, t_e, and $F_0 - B$ will not decouple from those in t_0 and γ. These three quantities are relatively poorly determined, so the degradation of the precision could be significant if the asymmetry of the observations about the peak is sufficiently large. To quantify this effect, I imagine that the two observations take place at $t_\pm = t_0 + \delta t \pm (2/3)^{1/2} \beta t_e$. That is, their midpoint is displaced from t_0 by a time δt, but the separation between the observations is the same as in the optimal case (eq. [23]). [The effect of using a different separation can easily be judged from the (1,1) component; eq. (22).] Since the errors are a minimum for $\delta t = 0$, we expect that they will be quadratic in δt.

Figure 2 shows the ratio, f, of the true error in Δu_x to the naive error as a function of δt for $\beta = 0.2$, 0.3, 0.4, and 0.5.

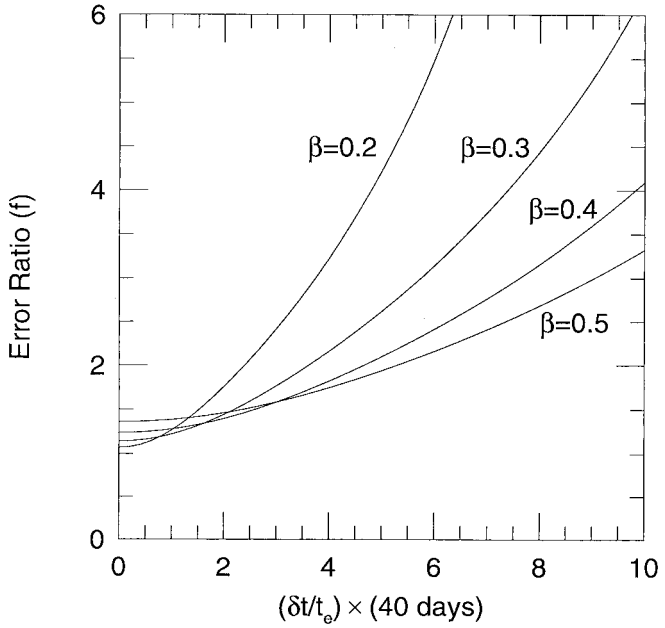

FIG. 2.—Ratio f of the actual error in Δu_x (taking full account of all the covariances among the 13 parameters of the full fit) to the naive error given by eq. (23) (together with the approximations that the error in Δu_x is equal to the error in $\Delta t_0/t_e$ and that the latter is dominated by the error in $t_{0,S}/t_e$). This ratio is shown for various values of the impact parameter β as a function of δt. Here δt is the time difference between the peak of the event and the midpoint of the two observations by the satellite. If the two observations are symmetric about the peak ($\delta t = 0$), then $1 \leq f \leq 1.36$. However, the errors can increase dramatically for nonsymmetric observations, particularly for small β. Symmetric observations yield more precise results because the uncertainties in t_e, β, and $F_0 - B$ (which are all relatively large) are then decoupled from the uncertainties in t_0. The curves shown in the figure all assume an Earth-satellite separation $d = 0.2$ AU and Einstein crossing time of $t_e = 40$ days. However, for other values of $t_e \lesssim$ yr$/2\pi$ and $d \ll$ AU, the curves are qualitatively similar.

For definiteness, I have as before assumed $d = 0.2$ AU and $t_e = 40$ days. The error in Δu_x becomes seriously degraded if δt is more than about 2 days. The effect is worse for low β because the effective timescale $t_{\rm eff} = \beta t_e$ is shorter, so the asymmetry of the observations is more severe for fixed δt. This result emphasizes the importance of scheduling the observations to be as symmetric as possible. However, it also shows that the inevitable ~ 1 day errors in estimating $t_{0,S}$ will not seriously affect the precision.

If the satellite separation is reduced to $d = 0.1$ AU but t_e remains at 40 days, then the results shown in Figure 2 remain qualitatively the same. On the other hand, if d remains at 0.2 AU while t_e is reduced to 20 days, then all the curves rise about twice as rapidly. That is, the figure remains approximately accurate for all relevant values of d and t_e provided that the abscissa is labeled " $(\delta t/t_e) \times$ (40 days)."

3.5. *Constraining the Baseline*

The calculations of the previous section were somewhat idealized in that they assumed that the baseline $(F_0 + B)$ is known exactly. For satellite observations, such exaggerated precision would come at a very high cost. In fact, observations of the baseline need not be very intensive. This can be understood as follows. Let the fluxes measured on opposite sides of the peak be F_1 and F_2, and suppose that the measurements are nearly symmetric, so that $\Delta F \equiv F_1 - F_2 \ll F_* \equiv (F_1 + F_2)/2$. From the ground-based mea-

surements combined with equations (13)–(16) (plus the fact that $|\Delta \boldsymbol{u}| \ll 1$), one knows $t_{0,S}$, β_S, $t_{e,S}$, and γ_S to within a few percent, and hence one also knows A at the time of the observations with similar precision. The quantity that gives information about Δt_0 is $\delta A/A = \delta F/(AF_0)$. That is, uncertainty in the estimate of F_0 will degrade the precision of Δt_0 only if its fractional error is of the same order as or larger than the fractional error in Δt_0. Since the latter is not likely to be much lower than $\sim 20\%$, only a relatively crude measurement of F_0 is necessary. The near-peak measurements give $AF_0 + B$ fairly precisely, and the baseline gives $F_0 + B$. The error in the difference, $(A - 1)F_0$, will thus be of the same order as the error in the baseline. Since A is known relatively well, F_0 will be determined with similar fractional accuracy as the baseline. Thus the baseline measurement can be an order of magnitude or more less precise than the peak measurements.

I find numerically that if the baseline exposure time is equal to the exposure time for each of the near-peak observations, then the precision of the determination of Δu_x is affected by 1% or less. Even if the exposure time is reduced by a factor of 10, the precision of Δu_x is degraded by 10% or less. Thus the total required observation time is well approximated by the time required for the two near-peak observations.

4. PRACTICAL CONSIDERATIONS

Here I consider the problems of timely event recognition, signal-to-noise ratio (S/N), image analysis, telescope time requirements, and backgrounds.

4.1. *Event Recognition*

The event must be recognized sufficiently early for two reasons. First, the precision of the ground-based measurement of $\gamma_\oplus$ (and so Δu_y) depends critically on when the intensive follow-up observations begin. Second, the characteristics of the event (t_0, β, t_e, and F_0) must be sufficiently well understood from the initial ground-based follow-up observations to plan the satellite observations. These latter are, by their nature, target-of-opportunity observations and so will inevitably require some rescheduling. Moreover, given the rotation of instruments, there is only a $\frac{1}{3}$ probability that the IRAC camera will be scheduled for use at the optimal time for the first exposure and another, independent $\frac{1}{3}$ probability that it will be scheduled for use at the optimal time for the second exposure. Thus a complicated decision process will be necessary to balance the requirements of these observations with other aspects of the SIRTF mission, and it is important that sufficient information about the event be available to make a rational decision on a timely basis.

Early recognition presents a significant challenge for the proposed observations. At present, the MACHO collaboration alerts on events when they surpass magnification $A = 1.6$ ($u_{\rm init} = 0.75$) rather than $A = 1.34$ ($u_{\rm init} = 1$) (A. Becker 1998, private communication). Figure 3 compares the S/N function $S(\beta)$ (see eqs. [19] and [21]) for these two values of $u_{\rm init}$. It is clear from this figure that the S/N is severely degraded for $\beta \gtrsim 0.45$ at $u_{\rm init} = 0.75$. A closely related problem is that the optimal time for the initial satellite observation is at $u = (5/3)^{1/2}\beta = 1.29\beta$ (see eq. [23]). Thus for $\beta = 0.5$ the optimal time for the first satellite observation is at $u = 0.65$, which is only a time $0.15t_e \sim 6$ days after the present-day initial alert.

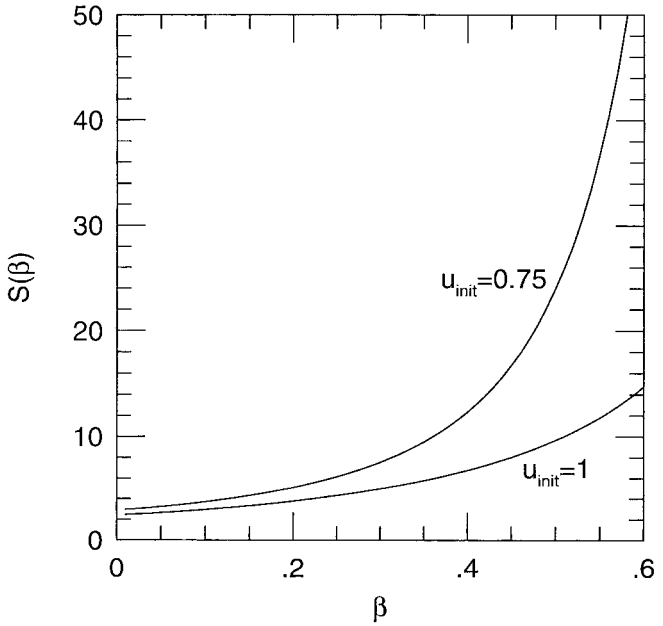

FIG. 3.—Normalized error S for the asymmetry parameter γ, which is used to determine Δu_y. See eqs. (12), (19), and (21). The lower curve assumes that intensive follow-up observations begin when the event enters the Einstein ring ($u_{\rm init} = 1$) and is the same as solid curve in Fig. 1. This curve is assumed in all calculations in the paper. The upper curve ($u_{\rm init} = 0.75$) reflects the present capability of the MACHO collaboration alert program. If this capability cannot be improved, the errors would increase substantially for $\beta \gtrsim 0.45$.

It is therefore important, although not absolutely critical, to alert on events earlier than the present standard. One approach would be to initiate aggressive follow-up observations at a lower threshold and to weed out the false alerts through these intensive observations. This would probably require a dedicated or nearly dedicated 1 m telescope. Another approach would be to obtain a higher S/N during the initial microlensing search observations. C. Stubbs (1998, private communication) and collaborators are trying to organize a search with a 2.5 m telescope, 1″ seeing, and a 1 deg^2 camera, which would represent a factor of 7 improvement in S/N relative to the present MACHO setup. It might well then be possible to alert on events at lower magnification. For example, the Optical Gravitational Lens Experiment (OGLE) collaboration web site[2] shows an event (OGLE-98-BULGE-24) with a maximum magnification of $A_{\rm max} \sim 1.3$. While the source for this event ($I \sim 16$) is much brighter than typical LMC events, this OGLE alert does show that with sufficient S/N it is possible to find events at lower magnification than those currently being achieved by MACHO. In any event, even if neither of these more aggressive programs are implemented, one could still carry out parallax measurements by restricting events to those with $\beta \lesssim 0.45$.

4.2. *Image Analysis*

I assume that the observations will be analyzed using image-differencing techniques that have been pioneered by Tomaney & Crotts (1996) and Ansari et al. (1997) to find microlensing events of unresolved stars in M31. Melchior et al. (1999), Tomaney (1998), and Alard & Lupton (1998) have further refined these techniques for application to photo-

[2] Located at http://www.astrouw.edu.pl/ftp/ogle/ogle2/ews/ews.html.

metry of *resolved* (or partially resolved) sources, such as those that are routinely monitored in the LMC, SMC, and the Galactic bulge. A version of the Alard-Lupton algorithm is now used by the Expérience Recherche d'Objects Sombres collaboration to make precise light-curve measurements for events found using their normal (more standard) photometry (Afonso et al. 1998).

The application of these techniques to the SIRTF IRAC camera should be relatively straightforward but not completely trivial. The pixel size of this camera is 1.2, while the point spread function (PSF) is about 2″. This is somewhat larger than the diffraction limit at 3.6 μm (with a 0.85 m telescope) of $\sim 1''$. However, the PSF will still be undersampled. The two exposures that are to be differenced will be separated by ~ 25 days and therefore rotated relative to one another by $\sim 25°$. Hence, the source star will not fall on exactly the same parts of the pixels in the two exposures. Variations in sensitivity across a single pixel would therefore make it impossible to obtain the required photometric precision (see § 4.3) by point-and-stare observations, so it will be necessary to dither the telescope by fractions of a pixel many times in order to enlarge the effective PSF and so smooth over the pixel-sensitivity variations.

The normal practice in image differencing is to form a "template image" by combining several images at baseline, then to subtract this from the event images. For the present case the procedure is quite different. The main information comes from directly differencing the two images taken symmetrically about the peak of the event. The shorter baseline exposure is *not* used as a template. Rather, the difference between this image and the average of the two images near peak is used to extract the less precise auxiliary information about F_0. See § 3.5.

I take note of a minor technical point. Image differencing automatically removes the background sources B from the analysis. This means that a standard microlensing light curve is fitted to four parameters rather than five. That is, one fits to

$$\tilde{F}(t; t_0, \beta, t_e, F_0) = F_0[A(t: t_0, \beta, t_e) - 1] , \qquad (24)$$

instead of equation (7). For this reason, it is sometimes mistakenly believed that the fit is less affected by the degeneracies associated with background light. Recall from § 2 that removal of these degeneracies is the central problem addressed by this paper. Why is equation (24) no more constraining than equation (7)? The latter can be formally rewritten as

$$F(t; t_0, \beta, t_e, F_0, \tilde{B}) = F_0[A(t: t_0, \beta, t_e) - 1] + \tilde{B} , \quad (25)$$

where $\tilde{B} \equiv F_0 + B$ is the baseline flux. In normal microlensing observations $\tilde{B}$ is extremely well determined because there are a large number of observations at baseline. Hence it is effectively decoupled from the other parameters in equation (25). On the other hand, $\tilde{F}$ in equation (24) refers to the flux *above baseline*. That is, equation (24) implicitly assumes that the baseline is well observed and that an essentially perfect template has been formed from these observations. Thus, in reality, equation (24) has the same information content as equation (7) or equation (25)

4.3. *Telescope Time*

I have already discussed at some length the requirements for the ground-based observations to measure $\gamma_\oplus$ and thus Δu_y (Gould 1998b). The basic result is summarized by equation (21). I focus here on the requirements for SIRTF observations.

In § 3.4 I introduced the quantity σ_*, the fractional photometry error for symmetric pair of observations near the peak. Recall that the error in Δu_x is given by $\sigma_{\Delta u_x} = (25/12)^{1/2} f\beta\sigma_*$, where f is the correction factor shown in Figure 2. For reasonably symmetric pairs of observations, $1 \le f \le 1.36$. The companion to equation (21) is then

$$\frac{\sigma_{\Delta u_x}}{\Delta u} = \left(\frac{25}{12}\right)^{1/2} f\beta\sigma_* \frac{\tilde{v}t_e}{d}$$

$$= 0.18 f \frac{\sigma_*}{0.01} \frac{\beta}{0.4} \frac{\tilde{v}}{275 \text{ km s}^{-1}} \frac{t_e}{40 \text{ days}} \times \left(\frac{d}{0.2 \text{ AU}}\right)^{-1} . \qquad (26)$$

Thus for a robust detection of parallax for a halo event with typical parameters requires $\sigma_* = 1\%$ photometry for two each of two observations near the peak plus a shorter exposure of the baseline (see § 3.5). This is to be compared with the ground-based requirement of 1% photometry, once per day for a period of $\sim 2.5 t_e$.

The IRAC detector records 0.7 e^- s^{-1} μJy^{-1}, and the sky plus dark current is expected to be 3 e^- s^{-1} pixel^{-1} (J. Hora 1998, private communication). The pixel size is 1.2. The PSF is expected to be 2″. However, I assume that the effective size of the PSF is increased to 3″ by dithering (see § 4.2). These figures imply that the background is $\sim 45\, e^-$ s^{-1}.

For the great majority of events detected to date, the source star is $V \ge 20$. For illustration, I consider two $V = 20$ stars, a main-sequence star ($V - L = 0.3$), and a clump giant ($V - L = 2.5$). I assume that 1 μJy corresponds to $L = 21.1$. For the main-sequence star, I find that the total exposure time required to reach $\sigma_* = 1\%$ precision is $T_{\rm exp} = 39(\beta^2 + 0.04\beta)$ hr. For the clump giant, the time required is $T_{\rm exp} = 0.6(\beta^2 + 0.33\beta)$ hr. Thus for main-sequence stars with $\beta \lesssim 0.4$, the total satellite time is $\sim 2T_{\rm exp} \lesssim 12$ hr, while for a red giant the time required is less than 1 hr. Clearly the latter is to be preferred. To date, unfortunately, only one LMC clump giant event has been published (Alcock et al. 1997a).

4.4. *Backgrounds*

As I have previously discussed (Gould 1998b), an asymmetric light curve can be the result of a binary lens or a binary source. I made a rough estimate that $\sim 20\%$ of events could be affected by such backgrounds that would lead to a spurious measurement of Δu_x. There are no backgrounds that would mimic a shift in the peak time as seen by the satellite relative to the Earth, assuming that the peaks were well resolved. Nevertheless, the method proposed here is to determine the peak from a pair of symmetrically placed observations. Thus the same asymmetry that produces a spurious detection of $\gamma_\oplus$ could in principle produce a slight shift in $t_{0,S}$. However, γ is measured from the "wings" of the light curve, $(t - t_0)/t_e \sim \pm 1$ (Gould 1998b), while the peak is determined from observations at $(t - t_0)/t_e \sim \pm(2/3)^{1/2}\beta$. Since $\partial F/\partial\gamma \propto 0.5(t - t_0)^3$ while $\partial F/\partial t_0 \propto (t - t_0)^1$, the effect of any background on the t_0 determination will be $\sim \beta^2/3$ smaller than on the γ-determination. That is, it will most likely be negligible. Thus it would seem advisable to push the satellite observations so that $\sigma_{\Delta u_y} < \sigma_{\Delta u_x}$. If the asymmetry detected from the ground

is truly due to parallax, one should also be able to detect a time delay provided that the observations are sensitive enough. Thus the satellite observations provide a partial check on the reality of the ground-based detection of parallax.

5. OTHER LINES OF SIGHT

In this paper I have focused attention mainly on the LMC, partly for simplicity and partly because I consider it to be the most interesting line of sight scientifically. However, there are two other lines of sight for which one might want to obtain satellite parallaxes: the SMC and the Galactic bulge.

The scientific question regarding events detected toward the SMC is similar to that for LMC events: are the lenses in the halo or in the Magellanic Clouds? The major difference between the SMC and LMC is that the LMC lies almost exactly at the ecliptic pole, whereas the SMC lies about 25° from the pole. This difference in turn has two implications. First, the equations describing parallax become more complicated. See, for example, Gaudi & Gould (1997). The "parallax ellipse" becomes more flattened, making the parallax effects smaller and so more difficult to measure. However, since the flattening is only by a factor of $\cos 25^\circ \sim 0.9$, the effect is quite minor and can be ignored for our purposes. Second, SIRTF cannot observe the SMC for the full year, as it can the LMC. The telescope can only point between 80° and 120° from the Sun. Hence the SMC is only observable for $\sim 65\%$ of the year. This is not a major problem, but combined with the fact that the SMC is smaller than the LMC (and so has fewer source stars to monitor), it does mean that it will provide fewer opportunities for parallax measurements.

The bulge is qualitatively different. First, it lies very close to the ecliptic, which implies that it can be observed only for two 40 day intervals during the year. Second, the parallax ellipse is highly flattened. For example, Baade's Window lies only 6° from the ecliptic, so the ellipse is flattened by a factor of 10. This flattening will reduce the size of the parallax asymmetry by a factor of 10 in the summer and winter and will reduce the time delay between the Earth and satellite by a factor of 10 in the spring and fall (Gaudi & Gould 1997). Since the bulge is observable from SIRTF only during the spring and fall, it is the latter effect that is relevant. Thus equation (21) will be virtually unaffected, but equation (26) will be increased by a factor of 10. This degradation of the S/N is partially mitigated by the fact that bulge events tend to be shorter ($t_e \sim 10$ days rather than 40 days), but it is exacerbated by almost as large a factor because most of the lenses are expected to be in the bulge, implying that $\tilde{v} = (d_{os}/d_{ls})v \sim 800$ km s^{-1} (rather than 275 km s^{-1}). Thus the photometric precision required is increased by approximately a factor of 7. From the standpoint of S/N, this is not a major problem. The bulge is about 6 times closer than the LMC, so clump giants are about 36 times brighter. Hence the exposure time is formally only $T_{exp} = 0.3\beta$ hr. However, whether systematics will compromise photometry at the required 0.14% level remains an open question.

From a scientific standpoint, bulge parallaxes can address two principal questions. First, where are the lenses? The conventional wisdom is that most are in bulge. However, the same conventional wisdom predicts a much lower optical depth and many fewer short events than are actually observed. One would like some experimental confirmation of this wisdom. Second, what is the mass spectrum of the lenses? Again, the conventional wisdom is that the lensing events are due to normal stars in the bulge (and secondarily the disk) along the line of sight. However, the observed mass spectrum of bulge stars (Holtzman et al. 1998) does not seem to be able to explain the observed distribution of timescales (Han & Gould 1996). Han & Gould (1995) showed that parallax measurements could help constrain both the location and the mass spectrum of the lenses.

Even if the time differences Δt_0 are initially too small to measure, the situation will gradually improve with time, because the Earth-satellite distance d will gradually grow. This tends to increase Δt_0 in two distinct ways. First, of course, as the satellite gets farther from the Earth, it takes longer for a lens to move from one to the other (see eq. [26]). In addition, the satellite is constrained to observe the bulge not when it is spring or fall on Earth but when the Sun is near the vernal or autumnal equinox as seen from the satellite. As the satellite moves farther from the Earth, the Earth-satellite separation vector becomes less closely aligned with the direction of the bulge during these critical times that the bulge is observable. Unfortunately, these same changes also make it more difficult to measure the parallax asymmetry from the ground. Nevertheless, if it initially proves too difficult to measure bulge parallaxes, the situation should be reviewed periodically in light of ongoing experience.

6. CONCLUSIONS

The method previously developed for measuring microlens parallaxes by directly comparing Earth-based and satellite-based photometry will not work for SIRTF. The old method requires that both sets of observations be done in the same band in order to remove degeneracies in the parallax solution. The SIRTF L-band detector response cannot be mimicked from the ground because of atmospheric absorption and high background.

However, by combining ground-based measurements of the "parallax asymmetry" γ of a lensing event (due to the Earth's acceleration) with the observed difference Δt_0 in the peak times of the event as seen from the Earth and SIRTF, it is possible to measure the parallaxes of microlensing events seen toward the LMC. The parallax yields the projected velocity of the lens, $\tilde{\boldsymbol{v}} = (d_{os}/d_{ls})\boldsymbol{v}$, and so would reveal whether the lenses are in the Galactic halo or in the LMC itself.

The ground-based measurement requires $\sim 1\%$ photometry about once per day for about 2.5 Einstein crossing times, i.e., ~ 100 days. The space-based measurement requires two observations each with about 1% precision plus one additional lower quality measurement. The two 1% measurements should be spaced approximately symmetrically about the peak of the event, while the lower quality measurement is needed to constrain the baseline. For a main-sequence star ($V = 20$, $V - L = 0.3$), the total satellite time required is ~ 12 hr $(\beta/0.4)(d/0.2\ \mathrm{AU})^{-1}$, where β is the impact parameter and d is the Earth-satellite distance. For a clump giant ($V = 20$, $V - L = 2.5$), less than 1 hr is required.

Events must be alerted in real time and an improvement in the current magnification threshold ($A \sim 1.6$) for the alerts would be helpful but is not critical. Photometry

should be carried out using image differencing. Backgrounds due to binary lenses and binary sources are minor but not completely negligible.

Parallax measurements are also possible for SMC events. The major difference from the LMC is that the SMC can be observed for only 70% of the year. Parallax measurements of Galactic bulge microlensing events are substantially different. Formally, the telescope time requirements are less severe than toward the LMC primarily because the sources are substantially brighter. However, because the bulge lies near the ecliptic, the size of the parallax effect is substantially smaller than toward the LMC, and this may mean that small systematic errors will compromise the measurements.

I thank G. Fazio and M. Werner for numerous stimulating discussions and for their general enthusiasm for using SIRTF to obtain microlens parallaxes. I thank B. S. Gaudi for a careful reading of the manuscript. This work was supported in part by grant AST 97-27520 from the NSF and in part by grant NAG 5-3111 from NASA.

REFERENCES

Afonso, C., et al. 1998, A&A, 337, L17
Alard, C., & Lupton, R. H. 1998, ApJ, 503, 325
Albrow, M., et al. 1999, ApJ, 512, in press
Alcock, C., et al. 1995, ApJ, 454, L125
———. 1997a, ApJ, 486, 697
———. 1997b, ApJ, 490, 59
———. 1997c, ApJ, 491, L11
———. 1997d, ApJ, 491, 436
Ansari, R., et al. 1997b, A&A, 324, 843
Aubourg, E., et al. 1993, Nature, 365, 623
Bennett, D. 1998, ApJ, 493, L79
Bennett, D., et al. 1997, BAAS, 191, 8308
Fields, B. D., Freese, K., & Graff, D. S. 1998, NewA, 3, 347
Gaudi, B. S., & Gould, A. 1997, ApJ, 477, 152
Gould, A. 1992, ApJ, 392, 442
———. 1994, ApJ, 421, L75
———. 1995a, ApJ, 441, L21
———. 1995b, ApJ, 441, 77
———. 1998a, ApJ, 499, 728
Gould, A. 1998b, ApJ, 506, 253
Gould, A., Miralda-Escudé, J., & Bahcall, J. N. 1994, ApJ, 423, L105
Han, C., & Gould, A. 1995, ApJ, 447, 53
———. 1996, ApJ, 467, 540
Holtzman, J. A., Watson, A. M., Baum, W. A., Grillmair, C. J., Groth, E. J., Light, R. M., Lynds, R., & O'Neil, E. J. 1998, AJ, 115, 1946
Melchior, A.-L., et al. 1999, A&A, in press
Paczyński, B. 1986, ApJ, 304, 1
Palanque-Delabrouille, N., et al. 1998, A&A, 332, 1
Refsdal, S. 1966, MNRAS, 134, 315
Sahu, K. C. 1994, Nature, 370, 275
Tomaney, A. 1998, preprint (astro-ph/9801233)
Tomaney, A., & Crotts, A. P. S. 1996, AJ, 112, 2872
Udalski, A., Kubiak, M., Szymanski, M., Pietrzynski, G., Wozniak, P., & Zebrun, K. 1998, Acta Astron., 48, 431
Wu, X.-P. 1994, ApJ, 435, 66
Zaritsky, D., & Lin, D. N. C. 1997, AJ, 114, 2545
Zhao, H. 1998, MNRAS, 294, 139